

Application of SABO-VMD-KELM in Fault Diagnosis of Wind Turbines

Yuling HE*, Hao CUI

Department of Mechanical Engineering, North China Electric Power University, Baoding, Hebei, 071003, China

*Corresponding Author: Yuling HE, E-mail: heyuling1@163.com

Abstract

In order to improve the accuracy of wind turbine fault diagnosis, a wind turbine fault diagnosis method based on Subtraction-Average-Based Optimizer (SABO) optimized Variational Mode Decomposition (VMD) and Kernel Extreme Learning Machine (KELM) is proposed. Firstly, the SABO algorithm was used to optimize the VMD parameters and decompose the original signal to obtain the best modal components, and then the nine features were calculated to obtain the feature vectors. Secondly, the SABO algorithm was used to optimize the KELM parameters, and the training set and the test set were divided according to different proportions. The results were compared with the optimized model without SABO algorithm. The experimental results show that the fault diagnosis method of wind turbine based on SABO-VMD-KELM model can achieve fault diagnosis quickly and effectively, and has higher accuracy.

Keywords: Wind turbine generator; Fault diagnosis; Subtraction-Average-Based Optimizer (SABO); Variational Mode Decomposition (VMD); Kernel Extreme Learning Machine (KELM)

1 Introduction

Wind energy has the characteristics of clean, environmental protection, large reserves and wide distribution^[1]. It has become one of the indispensable energy sources in today's world, and wind turbines are also all over the world. Due to its poor working conditions and complex load conditions, in order to ensure the normal operation of the wind turbine and reduce the cost of operation and maintenance, it is necessary to overhaul the wind turbine regularly. Wind turbine fault types can be divided into electrical faults and mechanical faults, and air gap eccentricity^[2] and inter-turn short circuit faults^[3] are the fault types with high frequency in mechanical and electrical faults, respectively. Wind turbine fault will have a significant impact on safe and efficient production, so the research on fault diagnosis method of wind turbine is of great significance to ensure the steady operation of wind turbine and equipment maintenance.

The generator fault signal is often accompanied by periodic impact, showing nonlinear and non-stationary characteristics. A large number of scholars have studied its fault diagnosis method^[4-7]. In literature^[8], the deep convolutional network is used to extract the vibration signal features of wind turbine, and then the fault

classification is completed through the fully connected neural network. The results show that the fault diagnosis rate of this method is higher than that of other comparison methods. Jing Huang and Ruping Lin^[9] et al. used whale optimization algorithm to optimize variational mode decomposition (VMD) with sample entropy as their fitness function, and then extracted the optimal intrinsic mode functions (IMFs) energy entropy to realize the generator inter-turn short circuit fault diagnosis, which improved the accuracy of fault diagnosis. Kernel Extreme Learning machine (KELM) is an extension of extreme learning machine, which can deal with nonlinear problems efficiently. Literature^[10] use the particle swarm optimization kernel extreme learning machine to diagnose the fault of rotating machinery, and a modified hierarchical multi-scale dispersion entropy calculation method is proposed. The results show that this methods can well complete the fault diagnosis of rotating machinery. The above scholars have proved the effectiveness of VMD and KELM in generator signal processing, but the selection of VMD and KELM parameters has a great impact on their result^[11]. Yong Lv^[12] proposed a VMD optimization algorithm based on variable bandwidth control parameter strategy and center frequency adaptive convergence strategy. The actual case verifies that the optimized VMD can obtain more accurate and efficient results.

Pavel Trojovsky and Mohammad Dehghani proposed the Subtraction-Average-Based Optimizer (SABO) [13] algorithm which is a mathematical metaheuristic algorithm based on mathematical concepts, foundations and operations in 2023. This method has fast convergence speed and good optimization results. This can prevent the dependence of the algorithm on specific middle group members, and through the optimization of this algorithm, it can avoid falling into local optimal solutions.

This paper proposes a wind turbine fault diagnosis method based on SABO-VMD-KELM model. Firstly, the SABO algorithm was used to optimize the VMD parameters to obtain the best modal components, and the features of the modal components were calculated to form a feature vector, and the training set and the test set were divided according to different proportions. Secondly, the SABO algorithm was used to optimize the KELM parameters by using the error rate of the training set and the test set as the fitness function, and the SABO-KELM model was established. Finally, the test set data is input for fault diagnosis and classification.

2 Fault Diagnosis Methods

2.1 Basic Principle of SABO

Unlike group-based metaheuristic algorithms inspired by various natural collective phenomena, the SABO algorithm is a mathematical metaheuristic algorithm based on mathematical concepts, foundations, and operations. This method features fast convergence and effective optimization results. The specific principles of the SABO algorithm are as follows:

(1) The search agent positions are randomly initialized in the search space.

$$x_{i,d} = lb_d + r_{i,d} \cdot (ub_d - lb_d) \quad i = 1, \dots, M \quad d = 1, \dots, n \quad (1)$$

$x_{i,d}$ is its d th dimension in the search space (decision variable), M is the number of search agents, n is the number of decision variables, $r_{i,d}$ is a random number between 0 and 1, and lb_d and ub_d are the lower and upper bounds of the d th decision variable.

(2) The iterative process of SABO.

The SABO algorithm is based on a newly proposed operation “ \bar{v} ”, which is defined by the \bar{v} -subtraction of the search agents Q from the search agent P , which is shown as follows:

$$P \bar{v} Q = \text{sign}(F(P) - F(Q))(P - \bar{v} * Q) \quad (2)$$

where \bar{v} is a vector of the dimension n , in which components are random numbers that are generated between 0 and 1, the operation “ $*$ ” represents the Hadamard product of the two vectors, $F(P)$ and $F(Q)$ are the values of the objective function of the search agents P and Q .

In the SABO method we've proposed, the movement of a given search agent X_i within the exploration space is determined by averaging the differences between every

other search agent X_j (where j equals 1, 2, ..., M) and the search agent X_i . Therefore, each search agent's updated location is computed using equation (3).

$$X_i^{new} = X_i + \bar{r}_i * \frac{1}{N} \sum_{j=1}^M (X_i - \bar{v} X_j) \quad i = 1, 2, \dots, M \quad (3)$$

where X_i^{new} is the new proposed position for the i th search agent X_i , M is the total number of the search agents, and \bar{r}_i is a vector of the dimension n , in which components have a normal distribution with the values from the interval $[0, 1]$.

Then, if this proposed new position leads to an improvement in the value of the objective function, it is acceptable as the new position of the corresponding agent, according to (4).

$$X_i = \begin{cases} X_i^{new} & F_i^{new} < F_i \\ X_i & \text{else} \end{cases} \quad (4)$$

where F_i and F_i^{new} are the objective function values of the search agents X_i and X_i^{new} , respectively.

2.2 VMD basic principles and optimization methods

Variational Mode Decomposition is an adaptive signal processing algorithm for handling non-stationary and nonlinear signals. It can determine the central frequency and bandwidth of each intrinsic mode function (IMFs) of the signal under a variational constraint framework, with the total bandwidth being minimal. The number of components is determined by the predefined number of decomposition levels K , then transforming the decomposition process of the original signal into the solving process of a variational problem. The specific steps are as follows:

(1) obtain the unilateral spectrum of IMFs.

$$A = [\delta(t) + j/\pi t] * u_k(t) \quad (5)$$

Where $k = 1, 2, \dots, K$, $\delta(t)$ is the impulse function, and $u_k(t)$ is the k -th IMF obtained from decomposition.

(2) Adjust the IMF spectrum to its fundamental band.

Introducing the exponential operator $e^{-j\omega_k t}$ to adjust the spectra of each modal component to their fundamental frequency band B .

$$B = [(\delta(t) + j/\pi t) * u_k(t)] e^{-j\omega_k t} \quad (6)$$

Where ω_k is the center frequency of the k th IMF.

(3) Demodulate each IMF, estimate the bandwidth of each modal component, and construct a constrained variational model.

$$\begin{cases} \min_{(u_k, \omega_k)} \left\{ \sum_{k=1}^K \left\| \partial_t [(\delta(t) + j/\pi t) * u_k(t)] e^{-j\omega_k t} \right\|_2^2 \right. \\ \left. \text{s.t. } P(t) = \sum_{k=1}^K u_k \right. \end{cases} \quad (7)$$

Where $\delta(t)$ is the Dirac distribution function and $\| \cdot \|_2$ is the 2-norm.

To solve the above constraint model, the quadratic

penalty factor and Lagrange multiplier are introduced, so that the constraint problem can be transformed into an unconstrained problem.

$$L(u_k, \omega_k, \lambda) = \alpha \sum_{k=1}^K \left(\left\| \partial t [(\delta(t) + j/\pi t) * u_k(t)] e^{-j\omega_k t} \right\|_2^2 \right) + \left\| P(t) - \sum_{k=1}^K u_k(t) \right\|_2^2 + \left\langle \lambda(t), P(t) - \sum_{k=1}^K u_k(t) \right\rangle \quad (8)$$

Where α is the quadratic penalty factor, and $\langle \cdot \rangle$ represents the inner product between vectors.

The central frequency method^[14] is usually used to determine the number of modal components in VMD. In this paper, the SABO algorithm is used to optimize the VMD's secondary penalty factor and the number of modal components K. The paper selects the minimum envelope entropy as the fitness function for VMD. Envelope entropy represents the sparsity characteristic of the original signal; when an IMF contains more noise and less characteristic information, the envelope entropy is higher, and vice versa. The fitness function serves as a criterion in the SABO-optimized VMD algorithm for evaluating the quality of search agent positions and is also an important factor influencing the quality of VMD results. The other parts of this paper are arranged as follows. Section II introduces the principle of fault diagnosis method, Section III summarizes the method process, and finally, the conclusion of this paper is obtained in the Section IV.

2.3 SABO-KELM

Kernel Extreme Learning Machine (KELM) is an improved algorithm based on Extreme Learning Machine (ELM) and optimized through a kernel function. KELM is capable of enhancing the predictive performance of the model while retaining the advantages of ELM. ELM is a single hidden layer feedforward neural network, whose objective function represented in matrix form is as follows.

$$F(x) = h(x)\beta = L \quad (9)$$

Where x is the input vector, $h(x)$ and H are the hidden layer node outputs, β is the output weight; L is the desired output.

Transform the network training into a problem of solving a linear system. It is determined according to the formula, where is the generalized inverse matrix of H . Introduce the regularization coefficient C and the unit matrix I to enhance the stability of the neural network. The least squares solution of β is shown in the formula(10-12).

$$\beta = H^* L \quad (10)$$

$$H^* = H^T (HH^T)^{-1} \quad (11)$$

$$\beta = H^T \left(\frac{I}{C} + HH^T \right)^{-1} L \quad (12)$$

In this paper, Radial-Basis-Kernel function is introduced into ELM, and the kernel matrix is shown in formula(13-15), where is the formula of Radial-Basis-Kernel function.

$$K(x_i, x_j) = \exp \left(-\frac{\|x_i - x_j\|^2}{\delta^2} \right) \quad (13)$$

$$\Omega_{KELM} = HH^T = h(x_i)h(x_j) = K(x_i, x_j) \quad (14)$$

The objective function can be expressed as:

$$F(x) = \begin{bmatrix} K(x, x_1) \\ \vdots \\ K(x, x_N) \end{bmatrix} \left(\frac{I}{C} + \Omega_{KELM} \right)^{-1} L \quad (15)$$

Where x_1, \dots, x_N is the given training sample, N is the number of samples.

This paper optimizes the regularization coefficient C and kernel coefficient of KELM using the SABO algorithm. The paper selects the error rate of the training and test sets as the fitness function for SABO-KELM.

3 Fault Diagnosis Process

Since the selection of parameters for VMD and KELM can impact their results, this paper uses the SABO algorithm to optimize the VMD secondary penalty factor, the number of modal components and the KELM kernel coefficient, regularization coefficient.

The main method process of this paper is shown in the figure, and the specific steps are as follows:

- (1) Decompose the original signal using VMD;
- (2) Set the number of iterations, optimization dimensions, and optimization bounds for the SABO algorithm, using the minimum envelope entropy as the fitness function, and apply the SABO algorithm to optimize the number of VMD modal components and the secondary penalty factor;
- (3) Obtain the optimal IMF and calculate its mean, variance, kurtosis, effective value, peak factor, impulse factor, dispersion entropy, permutation entropy, and sample entropy to construct a feature vector;
- (4) Set parameters for the SABO algorithm, and use the error rate of the training and test sets to optimize the regularization coefficient C and kernel coefficient of the KELM model;
- (5) Select the Radial-Basis-Kernel function as the kernel function for KELM, input the training set feature matrix to train the KELM model;
- (6) Input the test set data into the SABO-KELM model to obtain prediction results.

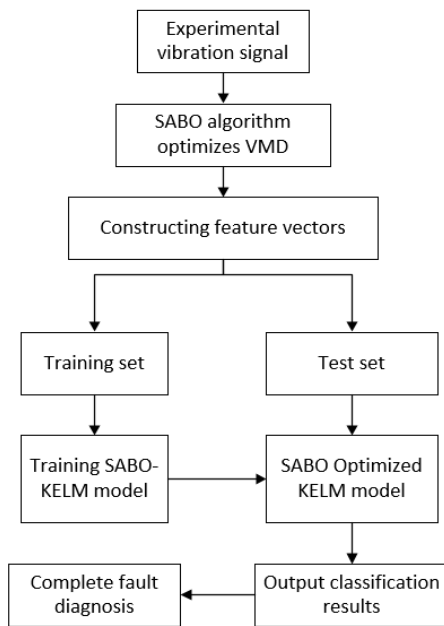


Figure 1 Flowchart of fault diagnosis

4 Experimental Analysis

4.1 Experimental signal acquisition

To verify the effectiveness of the proposed SABO-VMD-KELM model in this paper, experimental data from a LR-5 permanent magnet generator at North China Electric Power University is used. The test unit is an inner rotor permanent magnet wind power generator with a rated power of 5KW and a sampling frequency of 5000Hz. Simulations were carried out for four different states of the generator under full load operation: normal operation, 10% radial static eccentricity fault of the air gap (RSAGE), 10% short-circuit fault in stator windings between phases A1-A4 (SISC), and two combined faults (RSAGE & RISC). Vibration signals from the stator were collected using a vibration acceleration sensor. The table below shows some of the collected data.



Figure 2 Wind turbine experimental setup

4.2 Analysis of VMD results

Using SABO to optimize the VMD decomposition of stator vibration signals, obtaining the optimal IMF based on the minimum envelope entropy as the fitness function. Calculate its mean, variance, kurtosis, effective value, peak factor, impulse factor, dispersion entropy, permutation entropy, and sample entropy to construct a feature vector. Choose 100 signal groups under each of

the four conditions – normal, RSAGE, SISC, RSAGE&RISC (labeled as 1, 2, 3, 4, respectively) – totaling 400 signal groups as input and label them as shown in the table below. Due to space limitations, the table only lists the effective value from the feature vector. Figure 3 shows the distribution of the effective values of the best IMF components in each group, which can only roughly distinguish the four operating states of the generator, but cannot achieve accurate diagnosis, so it needs to be further imported into KELM for analysis.

Table 1 Grouping feature vectors

| Serial Number | Valid value | Label |
|---------------|-------------|-------|
| 1 | 2.5439 | 1 |
| ... | ... | ... |
| 100 | 3.5242 | 1 |
| 101 | 4.5712 | 2 |
| ... | ... | ... |
| 200 | 4.5803 | 2 |
| 201 | 3.2327 | 3 |
| ... | ... | ... |
| 300 | 2.7084 | 3 |
| 301 | 2.6484 | 4 |
| ... | ... | ... |
| 400 | 2.0802 | 4 |

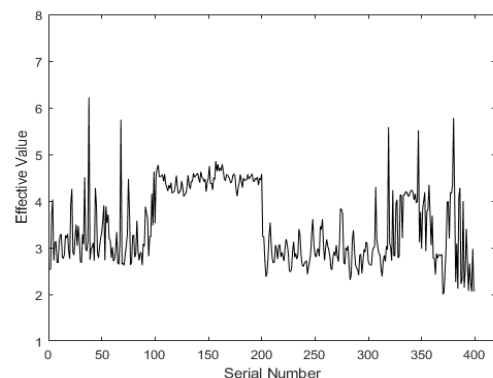


Figure 3 Effective value distribution of the best IMF components for each group

4.3 Analysis of KELM results

To validate the effectiveness of the SABO-VMD-KELM model in fault identification and the impact of the training set proportion on the results, training and test sets with different data partition ratios were randomly extracted. The test set was then input into the model for classification, and the results are presented in the table. The results demonstrate that as the proportion of the training set gradually increases, the accuracy of the model's recognition also improves. This proves the good stability of the SABO-VMD-KELM model, which does not suffer from overfitting or underfitting, though the model training time also increases. The figure below shows the confusion matrix when the training set accounts for 60%.

Table 2 Results for different test set proportions

| Percentage of training set | 30% | 40% | 50% | 60% |
|----------------------------|------|------|------|------|
| Accuracy/% | 93.2 | 95.6 | 96.8 | 98.1 |
| Testing time/s | 3.2 | 3.8 | 4.5 | 5.1 |

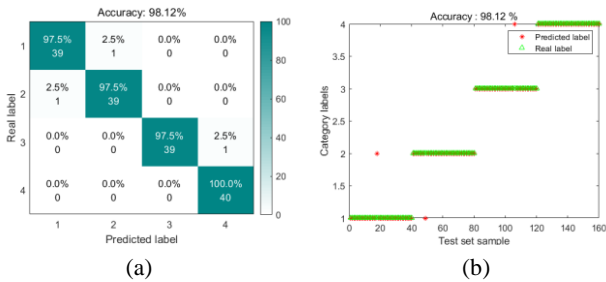


Figure 4 Fault diagnosis results

4.4 Comparison of methods

To further illustrate the effectiveness of the method in this paper, The SABO-KELM model is compared with the particle swarm optimization (PSO) KELM model, SABO-optimized VMD feature vectors were imported into SABO-KELM and PSO-KELM models, and the fault accuracy rates were calculated as shown in the figure. The table shows that SABO-VMD-KELM outperforms PSO-KELM in terms of accuracy for normal, RSAGE, SISC, and RSAGE&RISC conditions, and also has a shorter training time, demonstrating the effectiveness and speed of the method presented in this paper.

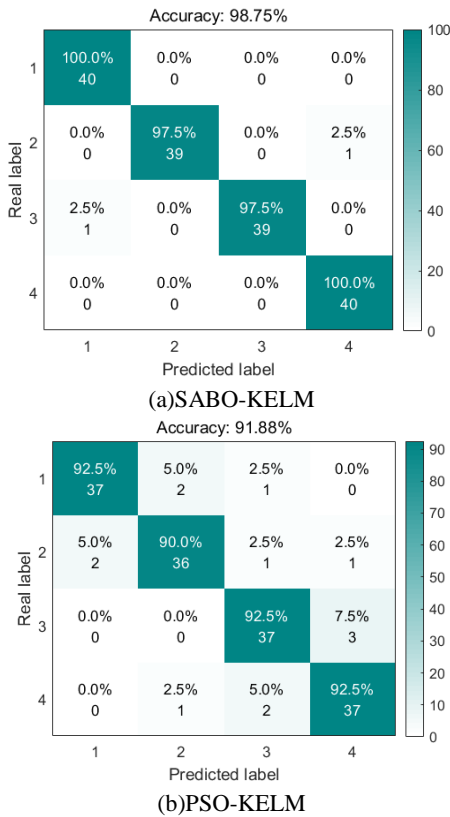


Figure 5 Comparison of method results

Both models were subjected to ten repeated

experiments, and the results showed that the correct diagnosis rate of SABO-VMD-KELM was consistently higher than that of PSO-KELM in all ten experiments.

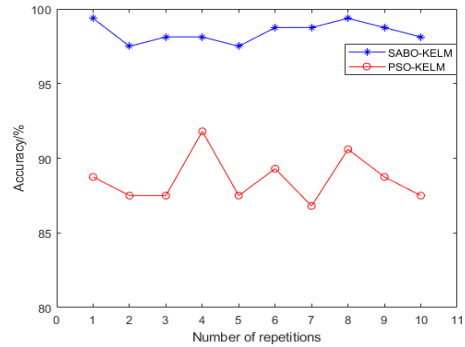


Figure 6 The results of ten times

Table 3 Accuracy comparison

| Method | Average accuracy/% |
|------------|--------------------|
| SABO -KELM | 98.75 |
| PSO-KELM | 91.88 |

5 Case Study of External Rotor Permanent Magnet Generator

5.1 Experimental signal acquisition

In order to further verify the effectiveness of the proposed method, the author uses the data of the outer rotor permanent magnet power generation motor model test unit for analysis. The following figure shows the experimental unit diagram of the outer rotor permanent magnet power motor model.

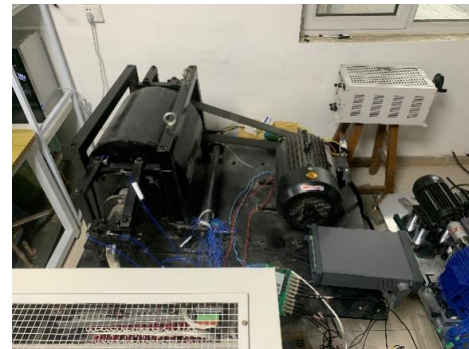


Figure 6 Outer rotor permanent magnet generator set

The moving-mode unit can simulate the external rotor permanent magnet generator RAGE, SISC, RSAGE&SISC, simulate the operation of external rotor permanent magnet generator by driving motor, and collect the vibration data of generator stator with sampling frequency of 5000Hz. The author recorded four kinds of generator fault data: normal, RSAGE, RISC, and RSAGE&SISC. The vibration data of each state was divided into 100 groups of signal sequences with length of 2048, a total of 400 groups of samples, and the proportion of training set and test set was 60%. The specific data information description is shown in the table:

Table 4 Data information description

| Type of fault | Number of training set groups | Lable |
|---------------|-------------------------------|-------|
| NORMAL | 40 | 1 |
| RSAGE | 40 | 2 |
| SISC | 40 | 3 |
| RSAGE&SISC | 40 | 4 |

5.2 Analysis of results

The author used SABO algorithm to optimize VMD parameters to extract the best IMF effective values for each group, and the results are shown in Figure 8.

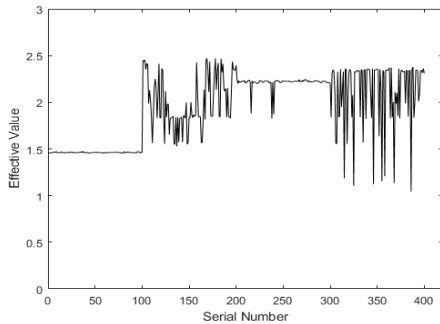


Figure 8 Effective value distribution of the best IMF components for each group

The characteristics of different faults in Figure 3 are slightly different and have a certain degree of identification, but precise fault diagnosis and classification cannot be achieved. Therefore, the extracted feature vectors are input into the SABO-KELM model for training and testing to obtain the fault diagnosis rate, and the results are shown in Figure 9.

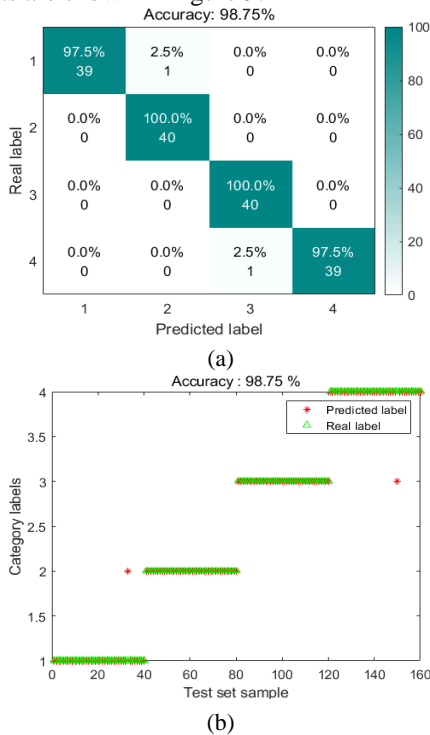


Figure 9 Fault diagnosis results

Only 2 of 160 groups of data were diagnosed incorrectly, and the accuracy of fault diagnosis reached 98.75%, which proved the effectiveness of the proposed method again.

6 Conclusion

In order to improve the fault diagnosis accuracy of wind turbine, this paper proposes a wind turbine fault diagnosis method based on SABO-VMD-KELM model. The conclusions are as follows:

(1) The SABO algorithm was applied to optimize the parameters of VMD and KELM, and the resulting SABO-VMD-KELM model achieved an average fault diagnosis accuracy rate of 98% for wind turbines. This demonstrates the effectiveness of the model in diagnosing faults in wind turbines and provides a reference method for research in fault diagnosis of wind turbines.

(2) Using the same SABO-optimized VMD to decompose the original signal data, the accuracy rate of SABO-KELM is higher than that of PSO-KELM, demonstrating that SABO-KELM has a clear advantage in terms of generalization performance and accuracy.

References

- [1] H. Polinder, J. A. Ferreira, B. B. Jensen, et al.. Trends in Wind Turbine Generator Systems [J]. IEEE Journal of Emerging and Selected Topics in Power Electronics, 2013,1(3):174-185.
- [2] Yu-Ling H. Impact of Static Air-Gap Eccentricity on Thermal Responses of Stator Winding Insulation in Synchronous Generators[J]. IEEE Transactions on Industrial Electronics, 2022,69(12):13544-13554.
- [3] Yu-Ling H. Impact of Stator Interturn Short Circuit Position on End Winding Vibration in Synchronous Generators [J]. IEEE Transactions on Energy Conversion, 2022,36(2):13544-13554.
- [4] M. Khov, J. Regnier and J. Faucher. Detection of turn short-circuit faults in stator of PMSM by on-line parameter estimation [C]. 2008 International Symposium on Power Electronics, Electrical Drives, Automation and Motion, 2008.
- [5] Z. Gao, S. X. Ding and C. Cecati. Real-time fault diagnosis and fault-tolerant control [J]. IEEE Transactions on Industrial Electronics, 2015,62(6):3752-3756.
- [6] T. Goktas, M. Zafarani and B. Akin. Discernment of Broken Magnet and Static Eccentricity Faults in Permanent Magnet Synchronous Motors [J]. IEEE Transactions on Energy Conversion, 2016,31(2):578-587.
- [7] J. -K. Park and J. Hur. Detection of Inter-Turn and Dynamic Eccentricity Faults Using Stator Current Frequency Pattern in IPM-Type BLDC Motors [J]. IEEE Transactions on Industrial Electronics, 2016,63(3):1771-1780.
- [8] Y. Shen, B. Chen, F. Guo, et al.. A Modified Deep Convolutional Subdomain Adaptive Network Method for Fault Diagnosis of Wind Turbine Systems [J]. IEEE Transactions on Instrumentation and Measurement, 2022,71:1-10.

- [9] J. Huang, R. Lin, Z. He, et al.. Application of WOA-VMD-SVM in Fault Diagnosis of Generator Inter-turn Short Circuit [C]. 2022 China Automation Congress (CAC),2022.
- [10] F. Zhou, J. Shen, X. Yang, et al.. Modified Hierarchical Multiscale Dispersion Entropy and its Application to Fault Identification of Rotating Machinery [J]. IEEE Access, 2020,8: 61361-161376.
- [11] X. Wang, G. Sui, J. Xiang, et al.. Multi-Domain Extreme Learning Machine for Bearing Failure Detection Based on Variational Modal Decomposition and Approximate Cyclic Correntropy [J]. IEEE Access, 2020,8: 97711-197729.
- [12] Y. Lv, Z. Li, R. Yuan, et al.. Variable-Bandwidth Self-Convergent Variational Mode Decomposition and its Application to Fault Diagnosis of Rolling Bearing [J]. IEEE Transactions on Instrumentation and Measurement, 2023,73:1-15.
- [13] Trojovský, P., Dehghani. Subtraction-Average-Based Optimizer: A New Swarm-Inspired Metaheuristic Algorithm for Solving Optimization Problems[J]. Biomimetics, 2023,8(1):149-152.
- [14] C. Wang, H. Li, G. Huang, et al.. Early Fault Diagnosis for Planetary Gearbox Based on Adaptive Parameter Optimized VMD and Singular Kurtosis Difference Spectrum [J]. IEEE Access, 2019,7:31501-31516.